Group velocity in lossy periodic structured media

P. Y. Chen, R. C. McPhedran, and C. M. de Sterke
IPOS and CUDOS, School of Physics, University of Sydney, NSW 2006, Australia

C. G. Poulton, A. A. Asatryan, and L. C. Botten
CUDOS, School of Mathematical Sciences, University of Technology, Sydney, NSW 2007, Australia

M. J. Steel
MQ Photonics Research Centre, CUDOS, and Department of Physics and Astronomy, Macquarie University, Sydney, NSW 2109, Australia
(Received 18 February 2010; published 24 November 2010)

In lossless periodic media, the concept of group velocity is fundamental to the study of propagation dynamics. When spatially averaged, the group velocity is numerically equivalent to energy velocity, defined as the ratio of energy flux to energy density of modal fields. However, in lossy media, energy velocity diverges from group velocity. Here, we define a modal field velocity which remains equal to the complex modal group velocity in homogeneous and periodic media. The definition extends to the more general situation of modal fields that exhibit spatial or temporal decay due to lossy elements or Bragg reflection effects. Our simple expression relies on a generalization of the concepts of energy flux and density. Numerical examples, such as a two-dimensional square array of silver rods in vacuum, are provided to confirm the result. Examples demonstrate how the dispersion relation of the periodic structure, the properties of its modes, and their group velocities change markedly in lossy media.

DOI: 10.1103/PhysRevA.82.053825 PACS number(s): 42.25.Bs, 42.70.Qs, 42.79.Gn, 78.67.Pt

I. INTRODUCTION

Media constructed from periodic microstructured metallic elements have attracted significant research interest recently in the fields of plasmonics and metamaterials. An understanding of pulse propagation through such media is important to their utility in future applications. However, loss is an unavoidable feature of metallic materials at optical and infrared wavelengths. Loss is fundamental to, and substantially impacts, the dynamics of pulse propagation, and cannot be ignored. For a medium with a given material dispersion relation satisfying the Kramers-Kronig relations, both the real and imaginary parts of the dispersion relation need be considered to obtain physical pulse propagation results.

It is well established in the literature that loss plays a significant role in pulse propagation through complex media. For example, plasmonic interconnects are promising because of their high bandwidth and subwavelength modal confinement [1,2], and the dispersion relations of lossy and lossless structures differ. This difference is apparent even in the simple case of a surface mode of planar lossy Drude-model waveguides, where modes with group velocities near zero no longer exist when loss is not neglected [3,4]. In general, loss particularly impacts slow light modes of any structure. In the photonic crystal literature, material losses are known to limit the group index of slow light modes [5,6]. More recently, broadband slow light modes have been found in lossless planar metamaterial waveguides, but these disappear when loss is considered [7,8]. Loss also imposes limitations on the capabilities of metamaterial in other applications: Pendry's perfect lens cannot be realized, and only a subresolution superlens is possible [9], and ideal cloaking cannot be achieved in a lossy metamaterial [9].

That accounting for loss is required to achieve physical pulse propagation results is nowhere more apparent than in the fast light literature. In a fast light medium where material losses or gains are ignored, the transit of a pulse through the medium can be smaller than the vacuum light travel time, violating special relativity and causality [10]. However, in this circumstance, the occurrence of physical amounts of loss or gain reshapes the pulse, ensuring propagation dynamics still obey relativity [11,12]. In all these examples, the imaginary part of a Kramers-Kronig-consistent dispersion relation significantly contributes to the physics of pulse propagation and cannot be neglected.

In lossless periodic media, the pulse propagation velocity is determined by the group velocity and the energy velocity. The utility of the group and energy velocities stems from the ability to calculate these quantities from the band diagram or waveguide dispersion relation and modal fields, respectively. The group velocity is defined by

$$\boldsymbol{v}_g = \nabla_{\boldsymbol{k}}\omega, \tag{1}$$

where ω and $\boldsymbol{k}$ are connected by the structure's dispersion relation, $\omega = \omega(\boldsymbol{k})$. In homogeneous media, the energy velocity is defined as the ratio of energy flux to energy density,

$$\boldsymbol{v}_E = \frac{\langle \boldsymbol{S} \rangle}{\langle U \rangle}, \tag{2}$$

where $\boldsymbol{S}$ is the time-averaged Poynting vector, and U is the time-averaged energy density. For periodic media, these quantities are defined by also spatially averaging over the unit cell.

In homogeneous lossless media, the group velocity is equivalent to the energy velocity,

$$\boldsymbol{v}_g = \boldsymbol{v}_E. \tag{3}$$

Yariv and Yeh have shown that this relation remains true in lossless periodic media [13]. These relations allow both pulse

propagation velocity and a structure's dispersion relation to be expressed in terms of the modal field distribution across the unit cell. These results apply even in the presence of material dispersion provided the loss is sufficiently small [10].

As in the examples discussed, loss has a physically significant impact on both pulse propagation and the band diagram. More subtle issues (a) whether group velocity still represents the pulse propagation velocity and (b) whether $\boldsymbol{v_g}$ and $\boldsymbol{v_E}$, as defined in (1) and (2), remain equivalent, as in (3). A brief discussion of (a) is given in Sec. II, along with alternatives to group velocity that predict pulse propagation dynamics in lossy media.

The main aim of this paper is to examine (b). This relation is not valid without modification when the modes used to calculate $\langle \boldsymbol{S} \rangle$ and $\langle U \rangle$ exhibit spatial or temporal attenuation, since energy dissipated by the propagation medium is now relevant. Redefining $\langle U \rangle$ to account for these transformations, as Loudon has done, means that (3) no longer holds [14]. The main result of this paper is a generalization of the ratio defined in (2), which can be calculated from the modal fields and remains numerically equal to the group velocity defined in (1). The result holds in systems where modal fields exhibit spatial or temporal decay, whether due to lossy elements in the structure or due to band gap effects in lossless periodic media. This is achieved by including both propagating and counterpropagating (adjoint) fields into the definitions of $\langle \boldsymbol{S} \rangle$ and $\langle U \rangle$. We term this new ratio the adjoint field velocity. Section II provides the motivation for this choice, and the derivation is presented in Sec. III.

Section IV discusses spatial and temporal decay of modes given by the imaginary parts of ω and k. It discusses the physical relevance of the freedom to choose between ω or k being complex and the impact of this choice on modal fields and band structures. The adjoint field velocity is shown to remain equal to the group velocity in both instances. Properties of counterpropagating modes in the context of the adjoint field velocity are presented. Technical issues arising from a complex vector $\boldsymbol{k}$ due to periodicity in two or more dimensions are discussed. Section V provides numerical examples to confirm the agreement between group velocity and the adjoint field velocity derived in Sec. III in lossless photonic crystals both in the band and the band gap and in a lossy silver photonic crystal. Appendix A presents a brief introduction to the *dual basis*, in which the adjoint modes reside. Appendix B contains a derivation of another ratio equivalent to the group velocity. It does not use adjoint fields, but we find that extra terms are required.

II. COMPLEX GROUP VELOCITY

In this section, we discuss group velocity in lossy periodic systems and its links to both pulse propagation and energy velocity. In particular, the equality between group velocity and the energy velocity, defined in (2), no longer holds, providing motivation for the adjoint field velocity.

In lossless periodic media, group velocity is unambiguously related to the time-domain pulse velocity. In lossy media, additional pulse propagation phenomena are observed, including pulse attenuation and peak reshaping. Meanwhile, $\boldsymbol{v_g}$, the change in ω due to an infinitesimal change in $\boldsymbol{k}$ along the dispersion relation $\omega(\boldsymbol{k})$, has both real and imaginary parts, requiring interpretation in terms of the aforementioned pulse propagation effects. Note that the complex nature of $\boldsymbol{v_g}$ bears no relation to the complex derivative of a complex analytic function, since, for example, $\boldsymbol{v_g}$ depends on the direction of $\boldsymbol{k}$.

Brillouin [10] and Loudon [14] have suggested that in the presence of significant loss the connection between group velocity, as defined in (1), and pulse propagation collapses. In highly lossy and dispersive media [15,16] or more recently in metamaterials [17,18], $d\omega/d[\mathrm{Re}(k)]$ often predicts a superluminal transit time, seemingly leading to the violation of relativity and causality. This has motivated Loudon to define a new energy velocity that remains subluminal, by accounting for not only the energy in the electromagnetic wave but also energy dissipated by the motion of particles in the lossy propagation medium. This energy velocity provides successful numerical predictions of pulse propagation [19].

However, the complex quantity $d\omega/dk$ remains linked to pulse propagation. Garrett and McCumber have shown that $d\omega/d[\mathrm{Re}(k)]$ still gives the velocity of the time-domain peak of a Gaussian pulse, even when $d\omega/d[\mathrm{Re}(k)]$ is superluminal [12].

These findings have been experimentally confirmed [15,16]. Others have identified the imaginary part of $d\omega/dk$ as a measure of the shift in the carrier frequency of a Gaussian pulse [20]. If $d\omega/dk$ is known over a broad frequency range, then the real and imaginary parts of $d\omega/dk$ correspond to propagation velocity and pulse reshaping, respectively [21].

We now turn to the connection between group velocity and energy velocity, with the energy velocity being defined in (2). Specifically, for a mode in a band of a lossless structure periodic in one dimension (1D),

$$v_E = \frac{l\mathcal{F}}{\mathcal{N}}, \tag{4}$$

where l is the length of the unit cell and $\mathcal{F}$ corresponds to the modal energy flux through the unit cell,

$$\mathcal{F} = \frac{1}{2}\int \mathrm{Re}(\boldsymbol{E} \times \bar{\boldsymbol{H}}) \cdot \hat{\boldsymbol{n}}\, ds, \tag{5}$$

and is thus integrated over one face of the unit cell. $\mathcal{N}$ is the modal energy density,

$$\mathcal{N} = \frac{1}{4}\int (\epsilon |\boldsymbol{E}|^2 + \mu |\boldsymbol{H}|^2)\, d\boldsymbol{x}, \tag{6}$$

integrated over the entire unit cell. The ratio $l\mathcal{F}/\mathcal{N}$ has dimensions of velocity. In dispersive media where material loss is small enough to be neglected, $\mathcal{N}$ requires modification,

$$\mathcal{N} = \frac{1}{4}\int \left(\frac{d(\epsilon\omega)}{d\omega} |\boldsymbol{E}|^2 + \frac{d(\mu\omega)}{d\omega} |\boldsymbol{H}|^2 \right) d\boldsymbol{x}, \tag{7}$$

as shown by Brillouin [10].

When material loss is introduced, these expressions no longer apply, since there is a transformation of energy carried by the electromagnetic wave into energy that is dissipated by the medium. Since $l\mathcal{F}/\mathcal{N}$ as defined here no longer includes all the energy transformations, it no longer results in correct values for v_g. This can be illustrated for homogeneous media by inserting plane waves with a complex ω or complex k into (5) and (6).

In the approach of Loudon, the energy density, $\mathcal{N}$, is defined to include terms due to forced oscillations of particles resulting from field interactions within the propagation medium [14]. The definition of energy flux is unchanged. The v_E associated with this definition is no longer equivalent to v_g, and the connection between modal field distributions and the band diagram or waveguide dispersion relation is lost. Furthermore, v_E no longer depends only on electromagnetic properties of the medium: An explicit model (Drude, Lorentz oscillator, etc.) of the material is required. The resulting v_E can vary depending on the details of the dispersion model used [22,23].

We define a velocity calculated from the modal fields which remains equivalent to v_g. We demonstrate that the definitions of flux and density in (4) fail to achieve equivalence with v_g because the modal fields experience decay. The source of this decay may be either due to lossy elements within the unit cell or due to Bragg reflection effects in a lossless photonic crystal. Instead, $\mathcal{F}$ and $\mathcal{N}$ will be defined as a product of modes and their corresponding counterpropagating modes, specifically, modes where $\boldsymbol{k} \to -\boldsymbol{k}$. Since the attenuation of these modes are in opposing directions, the product compensates for spatial field attenuation. This achieves a generalization of the role of energy velocity to modes that experience decay. The definition reduces to the energy velocity for nondecaying modes, but it diverges from Loudon's definition of energy velocity for decaying modes, as it retains equivalence with the group velocity.

Mathematically, combinations of propagating and counterpropagating fields correspond to modes from a basis and its dual, or equivalently, combinations of modes and adjoint modes. This was shown by Botten *et al.* in the context of diffraction gratings [24]. The use of the dual basis is motivated by the loss of Hermiticity when ϵ and μ are complex [25]. Eigenmodes of a non-Hermitian operator lack orthogonality and completeness properties. Inclusion of the dual basis establishes a complete biorthonormal basis [24,26]. A brief introduction to the dual basis and adjoint fields is given in Appendix A.

III. DERIVATION OF ADJOINT FIELD VELOCITY

In this section, we derive a relation between group velocity and energy velocity in a periodic medium:

$$\frac{d\omega}{dk} = \frac{l\mathcal{F}}{\mathcal{N}}. \tag{8}$$

Energy velocity, $l\mathcal{F}/\mathcal{N}$, is calculated from products of field quantities $\boldsymbol{E}$ and $\boldsymbol{H}$ that correspond to energy flux and energy density. Using adjoint fields defines the adjoint field velocity, providing the extension to the general case of modes that experience attenuation across the unit cell due to loss or Bragg reflection effects, defining an adjoint field velocity that remains equivalent to group velocity.

A. Lossless dispersive media

We begin with the simple case of a lossless periodic medium in the band, since the structure of the derivation is similar to the general lossy case. Material dispersion is permitted, but loss must be negligible so that ω and k can be assumed real. We arrive at a result which is identical to that of Joannopoulos [25]. We begin with the vector identity

$$\nabla \cdot (\boldsymbol{E_1} \times \bar{\boldsymbol{H}}_{\boldsymbol{2}}) = \bar{\boldsymbol{H}}_{\boldsymbol{2}} \cdot (\nabla \times \boldsymbol{E_1}) - \boldsymbol{E_1} \cdot (\nabla \times \bar{\boldsymbol{H}}_{\boldsymbol{2}}), \tag{9}$$

where $\boldsymbol{E_1}$ and $\boldsymbol{H_2}$ are time harmonic fields [$\boldsymbol{E} = \boldsymbol{E_0}(\boldsymbol{x})e^{-i\omega t}$] belonging to modal fields at two different frequencies, ω_1 and ω_2. The bar denotes complex conjugation. Inserting Maxwell's curl equations, we find

$$\nabla \cdot (\boldsymbol{E_1} \times \bar{\boldsymbol{H}}_{\boldsymbol{2}}) = i\omega_1\mu_1 \boldsymbol{H_1} \cdot \bar{\boldsymbol{H}}_{\boldsymbol{2}} - i\omega_2\epsilon_2 \boldsymbol{E_1} \cdot \bar{\boldsymbol{E}}_{\boldsymbol{2}}, \tag{10}$$

where μ_2 and ϵ_1 denote the quantities at ω_2 and ω_1, respectively. We exchange the subscripts, $1 \to 2$ and $2 \to 1$, and complex conjugate to give

$$\nabla \cdot (\bar{\boldsymbol{E}}_{\boldsymbol{2}} \times \boldsymbol{H_1}) = -i\omega_2\mu_2 \boldsymbol{H_1} \cdot \bar{\boldsymbol{H}}_{\boldsymbol{2}} + i\omega_1\epsilon_1 \boldsymbol{E_1} \cdot \bar{\boldsymbol{E}}_{\boldsymbol{2}}. \tag{11}$$

If ϵ and μ are nondispersive, we add (10) and (11) to obtain

$$\begin{aligned} &\nabla \cdot (\boldsymbol{E_1} \times \bar{\boldsymbol{H}}_{\boldsymbol{2}} + \bar{\boldsymbol{E}}_{\boldsymbol{2}} \times \boldsymbol{H_1}) \\ &\quad = i(\omega_1 - \omega_2)[\epsilon \boldsymbol{E_1} \cdot \bar{\boldsymbol{E}}_{\boldsymbol{2}} + \mu \boldsymbol{H_1} \cdot \bar{\boldsymbol{H}}_{\boldsymbol{2}}]. \end{aligned} \tag{12}$$

Since, in general $\epsilon_1 \neq \epsilon_2$ and $\mu_1 \neq \mu_2$, we first simplify (10) and (11) by expanding, in a Taylor series, $\omega_2\epsilon_2$ and $\omega_2\mu_2$ about $\omega_1\epsilon_1$ and $\omega_1\mu_1$,

$$\omega_2\epsilon_2 = \omega_1\epsilon_1 + (\omega_2 - \omega_1) \left.\frac{d(\epsilon\omega)}{d\omega}\right|_{\omega_1} + O\boldsymbol{(}(\omega_2 - \omega_1)^2\boldsymbol{)}, \tag{13}$$

and similarly for μ. On neglecting terms of $O\boldsymbol{(}(\omega_2 - \omega_1)^2\boldsymbol{)}$, these expansions imply

$$i\omega_1\epsilon_1 - i\omega_2\epsilon_2 = i(\omega_1 - \omega_2) \left.\frac{d(\epsilon\omega)}{d\omega}\right|_{\omega_1}, \tag{14}$$

$$i\omega_1\mu_1 - i\omega_2\mu_2 = i(\omega_1 - \omega_2) \left.\frac{d(\mu\omega)}{d\omega}\right|_{\omega_1}. \tag{15}$$

Now, adding (10) and (11) gives

$$\begin{aligned} &\nabla \cdot (\boldsymbol{E_1} \times \bar{\boldsymbol{H}}_{\boldsymbol{2}} + \bar{\boldsymbol{E}}_{\boldsymbol{2}} \times \boldsymbol{H_1}) \\ &\quad = i(\omega_1 - \omega_2)\left[\left.\frac{d(\epsilon\omega)}{d\omega}\right|_{\omega_1} \boldsymbol{E_1} \cdot \bar{\boldsymbol{E}}_{\boldsymbol{2}} + \left.\frac{d(\mu\omega)}{d\omega}\right|_{\omega_1} \boldsymbol{H_1} \cdot \bar{\boldsymbol{H}}_{\boldsymbol{2}} \right]. \end{aligned} \tag{16}$$

We integrate over the unit cell, denoted UC:

$$\begin{aligned} &\oint_{\partial \mathrm{UC}} (\boldsymbol{E_1} \times \bar{\boldsymbol{H}}_{\boldsymbol{2}} + \bar{\boldsymbol{E}}_{\boldsymbol{2}} \times \boldsymbol{H_1}) \cdot \hat{\boldsymbol{n}}\, ds \\ &\quad = i(\omega_1 - \omega_2) \int_{\mathrm{UC}} \left[\left.\frac{d(\epsilon\omega)}{d\omega}\right|_{\omega_1} \boldsymbol{E_1} \cdot \bar{\boldsymbol{E}}_{\boldsymbol{2}} \right. \\ &\qquad \left. + \left.\frac{d(\mu\omega)}{d\omega}\right|_{\omega_1} \boldsymbol{H_1} \cdot \bar{\boldsymbol{H}}_{\boldsymbol{2}} \right] d\boldsymbol{x}, \end{aligned} \tag{17}$$

where ∂UC denotes the boundary of the unit cell. To transform (17) into (8), we consider the limit as $\omega_2 \to \omega_1$. When ω_2 is infinitesimally close to ω_1, to first order, $\boldsymbol{E_1} \approx \boldsymbol{E_2}$ and $\boldsymbol{H_1} \approx \boldsymbol{H_2}$. This is justified in Appendix B. Then the right-hand side (RHS) of (17) is

$$\begin{aligned} \mathrm{RHS}(17) = i\Delta\omega \int_{\mathrm{UC}} \left[\frac{d(\epsilon\omega)}{d\omega} |\boldsymbol{E}|^2 + \frac{d(\mu\omega)}{d\omega} |\boldsymbol{H}|^2 \right] d\boldsymbol{x} \\ + O\boldsymbol{(}(\Delta\omega)^2\boldsymbol{)}, \end{aligned} \tag{18}$$

where $\Delta\omega = \omega_1 - \omega_2$, and the partial derivatives are evaluated at ω_1. The integrand can be recognized as being proportional to the electromagnetic energy density for a lossless medium, with corrections to account for material dispersion, first obtained by Brillouin [10].

The left-hand side (LHS) can be simplified using Bloch's theorem before applying any approximations, by expressing quantities on one face of the unit cell in terms of quantities on the opposing face. For a structure with 1D periodicity given by a lattice vector in the $\hat{\boldsymbol{x}}$ direction,

$$\begin{aligned}\mathrm{LHS}(17) = &-\int_{\mathrm{L}} (\boldsymbol{E_1}\times\bar{\boldsymbol{H}}_{\boldsymbol{2}} + \bar{\boldsymbol{E}}_{\boldsymbol{2}}\times\boldsymbol{H_1})\cdot\hat{\boldsymbol{x}}\, dy \\ &+\int_{\mathrm{R}} (\boldsymbol{E_1}\times\bar{\boldsymbol{H}}_{2} + \bar{\boldsymbol{E}}_{\boldsymbol{2}}\times\boldsymbol{H_1})\cdot\hat{\boldsymbol{x}}\, dy, \end{aligned} \tag{19}$$

integrating over the y coordinates of the unit cell, where subscripts L and R refer to the left and right faces of the unit cell. Applying Bloch's theorem, $\boldsymbol{E}_{\mathrm{R}} = \boldsymbol{E}_{\mathrm{L}} e^{ikl}$ and $\bar{\boldsymbol{E}}_{\mathrm{R}} = \bar{\boldsymbol{E}}_{\mathrm{L}} e^{-ikl}$, where k is the Bloch wave number, and l is the length of the unit cell, we get

$$\begin{aligned}\mathrm{LHS} &= (e^{i(k_1-k_2)l} - 1)\int_{\mathrm{L}} (\boldsymbol{E_1}\times\bar{\boldsymbol{H}}_{\boldsymbol{2}} + \bar{\boldsymbol{E}}_{\boldsymbol{2}}\times\boldsymbol{H_1})\cdot\hat{\boldsymbol{x}}\, dy \\ &= i(k_1-k_2)l\int_{\mathrm{L}} (\boldsymbol{E_1}\times\bar{\boldsymbol{H}}_{\boldsymbol{2}} + \bar{\boldsymbol{E}}_{\boldsymbol{2}}\times\boldsymbol{H_1})\cdot\hat{\boldsymbol{x}}\, dy \\ &\quad + O\boldsymbol{((\Delta}k)^2\boldsymbol{)} \\ &= i\boldsymbol{\Delta}kl\int_{\mathrm{L}} \mathrm{Re}(\boldsymbol{E}\times\bar{\boldsymbol{H}})\cdot\hat{\boldsymbol{x}}\, dy + O\boldsymbol{((\Delta}k)^2\boldsymbol{)}, \end{aligned} \tag{20}$$

where in the second equality a Taylor expansion of the exponential was used and terms of $O\boldsymbol{((\Delta}k)^2\boldsymbol{)}$ are neglected. In the third equality, fields are again assumed invariant to first order, neglecting higher order terms of $O\boldsymbol{((\Delta}k)^2\boldsymbol{)}$.

Following from (18) and (20), this allows the two sides of (17) to be equated,

$$\begin{aligned}&2\boldsymbol{\Delta}kl\int_{\mathrm{L}} \mathrm{Re}(\boldsymbol{E}\times\bar{\boldsymbol{H}})\cdot\hat{\boldsymbol{n}}\, dy \\ &= \Delta\omega\int_{\mathrm{UC}}\left[\frac{d(\epsilon\omega)}{d\omega}|\boldsymbol{E}|^2 + \frac{d(\mu\omega)}{d\omega}|\boldsymbol{H}|^2\right] d\boldsymbol{x}. \end{aligned} \tag{21}$$

Replacing $\frac{\Delta\omega}{\Delta k} \to \frac{d\omega}{dk}$ and rearranging gives (8), where $\mathcal{F}$ is given by (5) and $\mathcal{N}$ is given by (7). For nondispersive ϵ and μ, this reduces to (6). These formulas apply in the restricted case of a lossless dispersive material in the band since frequency ω and wave vector k were assumed to be real. Since $\mathcal{F}/\mathcal{N}$ is the ratio of energy flux to energy density, it is interpreted as the energy velocity [25].

B. Lossy dispersive media

We now provide a derivation of (8) in the general case of a lossy and dispersive system, which is the main result of this paper. The derivation mirrors the lossless case, which proceeded for two reasons: (a) Fields and conjugate fields both had frequency ω and (b) products of fields and conjugate fields (e.g., $|\boldsymbol{E}|^2$) had the same periodicity as the lattice. Periodicity is exhibited despite the modal fields only being quasiperiodic, accumulating a complex phase factor given by $\boldsymbol{k}$. Where ω is complex, conjugate fields now have frequency $\bar{\omega}$. Where $\boldsymbol{k}$ is complex, products of fields and conjugate fields are no longer periodic and also exhibit spatial decay.

Using adjoint fields resolves these issues. Products of propagating and counterpropagating fields remain periodic with the lattice. Furthermore, counterpropagating fields still have frequency ω, not $\bar{\omega}$. This allows the derivation to proceed as before with only minor adjustments. Mathematically, the counterpropagating mode is adjoint to the propagating mode. Modes and adjoint modes are related by [24]

$$\boldsymbol{E}^\dagger(\boldsymbol{x},\omega,\boldsymbol{k},\epsilon,\mu) = \boldsymbol{E}(\boldsymbol{x},\omega,-\boldsymbol{k},\epsilon,\mu), \tag{22}$$

where $\boldsymbol{E}^\dagger$ denotes the adjoint field. Fields and adjoint fields decay in opposing directions, and their product does not decay. This contrasts with the properties of the complex conjugate mode

$$\bar{\boldsymbol{E}}(\boldsymbol{x},\omega,\boldsymbol{k},\epsilon,\mu) = \boldsymbol{E}(\boldsymbol{x},-\bar{\omega},-\bar{\boldsymbol{k}},\bar{\epsilon},\bar{\mu}), \tag{23}$$

where complex conjugate fields are described by the Bloch vector $-\bar{\boldsymbol{k}}$ rather than $-\boldsymbol{k}$, and by frequency $-\bar{\omega}$ rather than ω. Despite these difficulties, an alternative derivation using the complex conjugate fields is given in the Appendix B to obtain v_g in the general case of a lossy dispersive periodic medium.

As before, we utilize the vector identity

$$\boldsymbol{\nabla}\cdot(\boldsymbol{E_1}\times\boldsymbol{H}_{\boldsymbol{2}}^\dagger) = \boldsymbol{H}_{\boldsymbol{2}}^\dagger\cdot(\boldsymbol{\nabla}\times\boldsymbol{E_1}) - \boldsymbol{E_1}\cdot(\boldsymbol{\nabla}\times\boldsymbol{H}_{\boldsymbol{2}}^\dagger). \tag{24}$$

Adding this to the equivalent of (11) and inserting Maxwell's equations give

$$\begin{aligned}&\boldsymbol{\nabla}\cdot(\boldsymbol{E_1}\times\boldsymbol{H}_{\boldsymbol{2}}^\dagger - \boldsymbol{E}_{\boldsymbol{2}}^\dagger\times\boldsymbol{H_1}) \\ &\quad = i(\omega_1-\omega_2)\left[\frac{d(\mu\omega)}{d\omega}\boldsymbol{H_1}\cdot\boldsymbol{H}_{\boldsymbol{2}}^\dagger - \frac{d(\epsilon\omega)}{d\omega}\boldsymbol{E_1}\cdot\boldsymbol{E}_{\boldsymbol{2}}^\dagger\right]. \end{aligned} \tag{25}$$

Since both sides vary in time as $\exp[-i(\omega_1+\omega_2)t]$, this common factor may be canceled. Further manipulation gives

$$\begin{aligned}&2\boldsymbol{\Delta}kl\int_{\mathrm{L}} (\boldsymbol{E_1}\times\boldsymbol{H}_{\boldsymbol{2}}^\dagger - \boldsymbol{E}_{\boldsymbol{2}}^\dagger\times\boldsymbol{H_1})\cdot\hat{\boldsymbol{n}}\, dy \\ &\quad = \boldsymbol{\Delta}\omega\int_{\mathrm{UC}}\left[\frac{d(\mu\omega)}{d\omega}\boldsymbol{H_1}\cdot\boldsymbol{H}_{\boldsymbol{2}}^\dagger - \frac{d(\epsilon\omega)}{d\omega}\boldsymbol{E_1}\cdot\boldsymbol{E}_{\boldsymbol{2}}^\dagger\right] d\boldsymbol{x}, \end{aligned} \tag{26}$$

Rearranging and replacing $\frac{\Delta\omega}{\Delta k} \to \frac{đ\omega}{đk}$, where the bar denotes a path-dependent derivative to distinguish it from the derivative of a complex analytic function, gives

$$\frac{đ\omega}{đk} = \frac{l\mathcal{F}}{\mathcal{N}}, \tag{27}$$

where

$$\mathcal{F} = \frac{1}{4}\int_{\mathrm{L}} (\boldsymbol{E}\times\boldsymbol{H}^\dagger - \boldsymbol{E}^\dagger\times\boldsymbol{H})\cdot\hat{\boldsymbol{n}}\, ds, \tag{28}$$

$$\mathcal{N} = \frac{1}{4}\int_{\mathrm{UC}}\left[\frac{d(\epsilon\omega)}{d\omega}\boldsymbol{E}\cdot\boldsymbol{E}^\dagger - \frac{d(\mu\omega)}{d\omega}\boldsymbol{H}\cdot\boldsymbol{H}^\dagger\right] d\boldsymbol{x}. \tag{29}$$

This result applies in the general case where ω, k, or both may be complex. In Section V we discuss some of the properties of adjoint fields and the quantities derived from these fields, $\mathcal{F}$ and $\mathcal{N}$. Section V gives two examples that are beyond the bounds of applicability of (5) and (7), but where (28) and (29) give the correct $đ\omega/đk$.

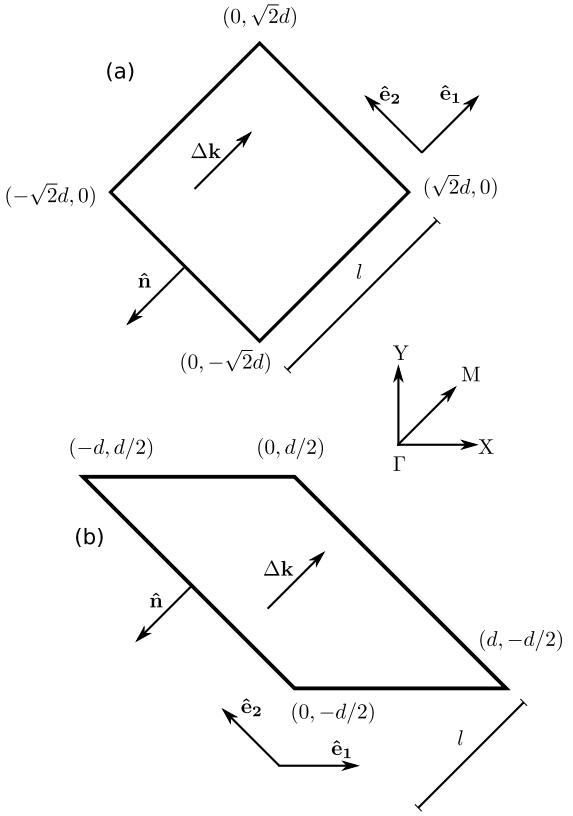

FIG. 1. Unit cell selected to simplify the calculation of $\mathcal{F}$ to a 1D calculation in a structure with 2D periodicity. Both (a) and (b) are appropriate choices for unit cells applying to a mode occupying the Γ-M segment of a square lattice. Vertex coordinates are shown, where d is the lattice parameter. The vector $\hat{\boldsymbol{n}}$ is normal to the chosen interface of the unit cell, where $\mathcal{F}$ is evaluated. The appropriate distance for (27) is l.

C. Two- or three-dimensional periodicity

For in-band modes of lossless periodic structures in two or three dimensions, Bloch modes are now described by a real vector $\boldsymbol{k}$. The 1D lossless result of (8) can still be used to calculate $\nabla_{\boldsymbol{k}}\omega$, in the direction $\boldsymbol{k}$, if the geometry of the unit cell is chosen appropriately. Issues arising from a complex vector $\boldsymbol{k}$ are discussed later. All but one of the basis vectors of the unit cell must be chosen to be orthogonal to $\boldsymbol{k}$. Then, (8) holds, with (5) being a line integral of the normal flux over one face of the unit cell that is parallel to the basis vectors orthogonal to $\boldsymbol{k}$. Figure 1 shows the choices of unit cell required for a mode along Γ-M in a two-dimensional (2D) square lattice. For example, for a mode of the square lattice along Γ-M, both a rotated square unit cell and a parallelogram-shaped unit cell are appropriate. The RHS(8) is an integral over the unit cell's area, and the LHS(8) is a line integral of the component of $\mathrm{Re}(\boldsymbol{E}\times\bar{\boldsymbol{H}})$ in the $\hat{\boldsymbol{n}}$ direction shown, on the chosen face of the unit cell.

This result follows from considering the surface integral in (17). Ordinarily, the integral contains contributions from two or three sets of opposing faces. All but one set of contributions can be canceled when the basis vectors of the unit cell are chosen such that $\Delta\boldsymbol{k}\cdot\boldsymbol{e_2}=\Delta\boldsymbol{k}\cdot\boldsymbol{e_3}=0$, where $\Delta\boldsymbol{k}$ is the difference in the Bloch wave number of modes 1 and 2 and $\boldsymbol{e_n}$ are the basis vectors. The integrand in (17) on opposing faces of the unit cell is then related through Bloch's theorem via the multiplicative factor $e^{i\Delta\boldsymbol{k}\cdot\boldsymbol{e}_n}=1$, where $n=2$ or 3. The integrands on opposing faces are equal and opposite, and thus they cancel. The definition of $\mathcal{F}$ reduces to the 1D case given in (5).

Furthermore, it is possible to use (8) and (5) to calculate $\nabla_{\boldsymbol{k}}\omega$ in any direction $\hat{\boldsymbol{k}}$, not just the direction of the Bloch wave number. Again, by returning to (17), eigenmodes $\boldsymbol{E_1}$ and $\boldsymbol{E_2}$ can be chosen such that $\Delta\boldsymbol{k}$ is in the direction $\hat{\boldsymbol{k}}$. Again the unit cell must be chosen such that $\Delta\boldsymbol{k}\cdot\boldsymbol{e_2}=\Delta\boldsymbol{k}\cdot\boldsymbol{e_3}=0$. The results hold as before.

Additional subtleties arise in lossy media since $\boldsymbol{k}$ is now a complex vector. We may consider the three spatial components of $\boldsymbol{k}$, each with real and imaginary parts. Alternatively, we may consider the spatial directions of the real and imaginary parts of $\boldsymbol{k}$, which may or may not be collinear. If collinearity is present, then the calculation of $\nabla_{\boldsymbol{k}}\omega$, based on (27), reduces to a 1D problem again by choosing all but one basis vectors of the unit cell to be perpendicular to $\boldsymbol{k}$. However, when collinearity is absent, no choice of basis vectors allows all but one basis vector to be perpendicular to both the real and imaginary parts of $\boldsymbol{k}$, and a reduction to a 1D problem is impossible. For the purpose of this paper, we only discuss propagation of modes where $\mathrm{Re}(\boldsymbol{k})$ and $\mathrm{Im}(\boldsymbol{k})$ are collinear. In Section IV, we discuss in detail factors that control the directions of the real and imaginary parts of $\boldsymbol{k}$, including the geometry of energy coupling into a periodic structure.

IV. PROPERTIES OF ADJOINT FIELDS

In this section, we discuss in greater detail the modes used in the definition of adjoint flux and density. We begin with a discussion of the impact of loss on Bloch modes of a periodic system due to ω or k being complex. We also discuss the effect of a complex $\boldsymbol{k}$ present in structures with periodicity in two or three dimensions.

A. Modes with complex ω or complex k

Until now, the modal fields of lossy periodic structures have not been discussed, except in terms of abstract properties such as quasiperiodicity. We show that the eigenmodes of a lossy structure are not unique and, depending on whether ω or k is complex, distinct sets of eigenmodes are obtained. The set of eigenmodes chosen is motivated by physical considerations.

We illustrate with the simple example of a lossy homogeneous medium. Let the monochromatic plane wave fields in a medium given by the dispersion relation $k^2=\epsilon\mu\omega^2$ propagating in the $\hat{\boldsymbol{z}}$ direction be described by

$$\boldsymbol{E}(\boldsymbol{x})=\hat{\boldsymbol{x}}e^{i(kz-\omega t)},\quad \boldsymbol{H}(\boldsymbol{x})=\hat{\boldsymbol{y}}\sqrt{\frac{\epsilon}{\mu}}e^{i(kz-\omega t)}. \tag{30}$$

The adjoint fields represent the solution propagating in the opposite direction, or $k\to -k$,

$$\boldsymbol{E}^{\dagger}(\boldsymbol{x})=\hat{\boldsymbol{x}}e^{-i(kz+\omega t)},\quad \boldsymbol{H}^{\dagger}(\boldsymbol{x})=-\hat{\boldsymbol{y}}\sqrt{\frac{\epsilon}{\mu}}e^{-i(kz+\omega t)}. \tag{31}$$

One or both of ω and k must be complex to satisfy the dispersion relation $k^2=\epsilon\mu\omega^2$, and ultimately the wave equation.

However, ω and k cannot be uniquely specified. In particular, ω may be chosen as real, forcing k to be complex, and vice versa. When ω is chosen as real, the fields in (30) decay as $e^{-\kappa z}$, where κ is the imaginary part of k, while the adjoint fields (31) grow as $e^{\kappa z}$. Field amplitudes are constant in time. When k is chosen as real and ω is complex, fields do not spatially decay but change uniformly in space as a function of time. A complete set of eigenmodes of the system is obtained by varying the real parameter from 0 to ∞, with the complex parameter determined by the dispersion relation.

From a mathematical perspective, the choices of ω or k being real are equally valid. For a given physical problem, however, one choice is more relevant than the other. The choice of ω real and k complex is more desirable when describing the propagation through passive media, for example modes of a waveguide, surface modes, or bulk modes of a photonic crystal. Energy is coupled into the mode, which subsequently decays as it propagates in space. Figure 2 shows an example where the lossy modes of a semi-infinite metallic photonic crystal are excited by a plane wave in semi-infinite free space. Modes of the photonic crystal are Bloch modes with a complex k. Typical boundary conditions can be applied at the interface to obtain coupling coefficients between the free space modes and the Bloch modes. The Bloch wave number k then describes phase advancement and attenuation of the field inside the passive medium.

Modes with complex ω and real k better describe time evolution of fields after an initial impulse in time. For example, electromagnetic energy may be inserted into a cavity mode, which then exhibits a characteristic decay time. The initial condition can be expressed as a linear superposition of modes, each described by a decay rate proportional to the imaginary part of ω. Real k is also appropriate under scenarios where fields are not subject to spatial decay, for example, a pumped lasing mode of an optical cavity. Here, the imaginary part of ω is related to the lasing threshold of the mode [27].

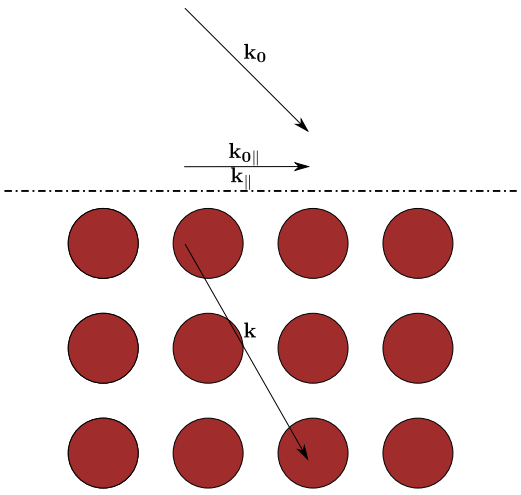

FIG. 2. (Color online) Boundary condition between semi-infinite free space and a semi-infinite 2D photonic crystal. A Bloch mode described by $\boldsymbol{k}$ is excited by a plane wave described by $\boldsymbol{k_0}$. Boundary conditions ensure that the parallel component of $\boldsymbol{k_{0\parallel}}$ is conserved from the plane wave to the Bloch mode, determining $\boldsymbol{k_\parallel}$.

B. Modes of 2D or 3D structures

As mentioned in Sec. III, structures with periodicity in two or three dimensions can be simplified to a 1D problem when the real and imaginary parts of $\boldsymbol{k}$ are collinear. We now discuss the conditions which result in Bloch modes described by $\boldsymbol{k}$ with the collinearity property. A Bloch mode's $\boldsymbol{k}$ is determined not only by the direction of propagation within the structure but by the nature of the coupling into the structure. We use the illustrative example of a semi-infinite lossy photonic crystal incident from above by a plane wave described by $\boldsymbol{k_0}$, where boundary conditions must be satisfied at the interface (Fig. 2). We refer to this interface as the cut plane of the crystal. The component of $\boldsymbol{k_0}$ parallel to the interface is conserved at the boundary between free space and the semi-infinite crystal [28] (i.e., $\boldsymbol{k_{0\parallel}} = \boldsymbol{k_\parallel}$), to within a reciprocal lattice constant. Furthermore, $\boldsymbol{k_\parallel}$ remains conserved throughout the semi-infinite crystal, and it is consequently identical at each successive layer of the photonic crystal. The $\boldsymbol{k_{0\parallel}}$ of the incoming plane wave therefore specifies $\boldsymbol{k_\parallel}$ of the Bloch mode within the crystal.

For an incident plane wave not spatially decaying, $\mathrm{Im}(\boldsymbol{k_{0\parallel}}) = \mathrm{Im}(\boldsymbol{k_\parallel}) = 0$. The Bloch mode does not spatially decay in the parallel direction. For a mode with real ω, spatial decay of a Bloch mode is present in a lossy medium, and any imaginary component of $\boldsymbol{k}$ must be perpendicular to the interface. If the incident plane wave has a nonzero component of $\boldsymbol{k_{0\parallel}}$, then $\boldsymbol{k_\parallel}$ is also nonzero. In this system, the real and imaginary parts of $\boldsymbol{k}$ are not collinear, since $\mathrm{Im}(\boldsymbol{k})$ is perpendicular to the cut plane, while $\mathrm{Re}(\boldsymbol{k})$ has a component parallel to the cut plane.

In summary, while the real and imaginary parts of $\boldsymbol{k}$ are connected by the dispersion relation, $\omega = \omega(\boldsymbol{k})$, the geometry of energy coupling into Bloch modes determines key aspects of $\boldsymbol{k}$. For bulk modes of 2D photonic crystals, the orientation of $\mathrm{Im}(\boldsymbol{k})$ is determined entirely by the cut plane, and the value of $\boldsymbol{k_\parallel}$ by the incident plane wave. In general, the real and imaginary parts of $\boldsymbol{k}$ can only be collinear if a normally incident plane wave is considered. The 1D result of (27) is restricted to modes with this collinearity property.

C. Properties of adjoint flux and density

We now turn our attention to the properties of adjoint fields in the context of the adjoint field velocity. First, we show that the simple fields of a homogeneous medium given by (30) and (31) produce the correct value of v_g when evaluated in terms of (27). The time dependence of these harmonic fields is ignored, having been factored out of the field quantities in $\mathcal{F}$ and $\mathcal{N}$. Although the adjoint field velocity is valid whether ω or k is complex, we choose to maintain ω real and k complex, as this is more suitable for describing propagation within the medium after coupling from free space modes. Due to the infinite translational symmetry, and since any product of fields and its adjoint fields is conserved in magnitude under translation in space, a unit cell of any size beginning at any origin can be chosen. Hence, $\mathcal{F} = 2\sqrt{\epsilon/\mu}$ and $\mathcal{N} = 2l\epsilon$, where l is the length of the unit cell in x. This gives $\bar{d}\omega/\bar{d}k = 1/\sqrt{\epsilon\mu}$, as expected.

This simple example displays four general properties of any Bloch mode under the adjoint formulation.

(i) *Integrands in* (28) and (29) *do not decay from one unit cell to the next.* Fields are always coupled with adjoint fields, with the opposing Bloch factor, $\boldsymbol{k} \to -\boldsymbol{k}$, decaying in the opposite direction. Flux $\mathcal{F}$ and density $\mathcal{N}$ are consequently fully periodic functions of space. As a result, the adjoint formulation need not explicitly deal with decaying electromagnetic fields due to dissipation of energy by the medium. Formulations of $\mathcal{F}$ and $\mathcal{N}$ based on complex conjugate quantities do not have this property in a lossy medium.

(ii) *The adjoint field velocity reproduces the energy velocity when ω and k are both real.* Specifically, $\mathcal{F}$ and $\mathcal{N}$, defined in (28) and (29), reduce to the equivalent complex conjugate quantities defined in (5) and (7). From the properties of complex conjugate and adjoint fields (23) and (22), these fields represent modes that differ only in the sign of ω. They satisfy the same vector Helmholtz equation,

$$(\nabla^2 + \epsilon_i \mu_i \omega^2)\boldsymbol{E} = \boldsymbol{0}, \tag{32}$$

in each region i, as the sign of ω is immaterial. Furthermore, they see identical ϵ and μ across the unit cell and satisfy the same boundary conditions. The conjugate and adjoint spatial $\boldsymbol{E}$ fields are identical. But by Faraday's law, $\nabla \times \boldsymbol{E} = -\partial \boldsymbol{B}/\partial t$, the conjugate and adjoint $\boldsymbol{H}$ fields differ by a minus sign due to the difference in the sign of ω. These properties allow the recovery of (5) and (7) from (28) and (29), collapsing the adjoint definitions of $\mathcal{F}$ and $\mathcal{N}$ to their complex conjugate counterparts.

(iii) *Fields and adjoint fields are related by symmetry, since these are the forward and backward propagating modes.* If the transformation $\boldsymbol{k} \to -\boldsymbol{k}$ accords with a symmetry of the lattice then symmetry arguments can be used to derive the adjoint field from the original field. The simple example given here and many 2D and 3D photonic crystal geometries contain inversion centers. Propagating through the structure with Bloch wave number $-\boldsymbol{k}$ is equivalent to propagation through the space inverted structure with Bloch wave number $\boldsymbol{k}$. The adjoint field is then obtained by following rules of $\boldsymbol{E}$ and $\boldsymbol{H}$ fields under an inversion operation [29],

$$\boldsymbol{E}^\dagger(\boldsymbol{x},\boldsymbol{k}) = \boldsymbol{E}(\boldsymbol{x},-\boldsymbol{k}) = -\boldsymbol{E}(-\boldsymbol{x},\boldsymbol{k}). \tag{33}$$

The first equality results from identifying the adjoint field as the backward propagating wave [24], while the second equality utilizes the inversion properties of $\boldsymbol{E}$ in three dimensions. The $\boldsymbol{H}$ field transforms as a pseudovector,

$$\boldsymbol{H}^\dagger(\boldsymbol{x},\boldsymbol{k}) = \boldsymbol{H}(\boldsymbol{x},-\boldsymbol{k}) = \boldsymbol{H}(-\boldsymbol{x},\boldsymbol{k}). \tag{34}$$

Therefore only the forward propagating mode needs to be explicitly calculated. In the following calculations, in Fig. 3, 5, and 8, the adjoint field velocity is calculated using these inversion properties.

(iv) *The values of $\mathcal{F}$ and $\mathcal{N}$ are not unique, but the ratio $\mathcal{F}/\mathcal{N}$ is unique.* In the complex conjugate formulation, (5) and (7), this is seen by scaling $\boldsymbol{E}$, and therefore $\boldsymbol{H}$, by any complex factor. The magnitudes of $\mathcal{F}$ and $\mathcal{N}$ scale by the square modulus of that factor, but the ratio $\mathcal{F}/\mathcal{N}$ remains unaffected. In the adjoint formulation, (28) and (29), scaling $\boldsymbol{E}$ by a complex multiplicative factor demonstrates that both the magnitude and complex phase of $\mathcal{F}$ and $\mathcal{N}$ are unconstrained. However, their ratio is similarly unaffected. In the former case, defining a mode to contain unit energy constrains $\mathcal{N}$. This is usually achieved by applying orthonormality of modes, $\langle \psi_i | \psi_j \rangle = \delta_{ij}$. A similar orthonormality may be applied to the adjoint formulation; however, this does not guarantee that the resulting $\mathcal{N}$ has the interpretation of energy density.

V. NUMERICAL EXAMPLES

In this section we present three numerical examples demonstrating the equivalence of group velocity and adjoint field velocity (27). The first example illustrates the properties of adjoint fields and the adjoint definitions of flux and density described in Sec. IV in a 1D periodic geometry. The second and third examples confirm the validity of (27) in situations where traditional definitions of energy flux and energy density fail: in the band gap of a lossless photonic crystal and in a lossy photonic crystal. Both are 2D examples. The third example deals with the omnidirectional flat bands observed in lossless metallic rods, ascribed to plasmon resonances.

We first consider propagation through a 1D photonic crystal at normal incidence. The unit cell is composed of vacuum and a lossy dielectric. Calculations are performed using the transfer matrix method [30]. The modal field E is plotted in Fig. 3, spanning 1.5 unit cells with two layers of dielectric and one layer of vacuum. The adjoint field $E^\dagger$ is obtained by a reflection of E about the inversion center at 0.75. The freedom to scale adjoint fields by a complex multiplicative factor is used to ensure that $(\epsilon E E^\dagger - \mu H H^\dagger)$ is a real quantity within the vacuum. The field E and adjoint field $E^\dagger$ decay in opposite directions with opposite quasiperiodicities, ensuring $(\epsilon E E^\dagger - \mu H H^\dagger)$ remains periodic and $(E H^\dagger - H E^\dagger)$ is constant. This demonstrates, for periodic media, that products of fields and their adjoints do not spatially decay and, in particular, the adjoint flux is conserved.

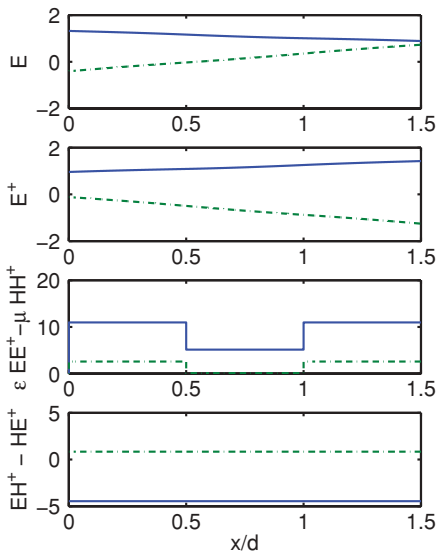

FIG. 3. (Color online) Field quantities of a 1D photonic crystal composed of two materials a and b, with dielectric constants $\epsilon_a = 4 + 4i$ and $\epsilon_b = 1$ and lengths $l_a = 0.5$ and $l_b = 0.5$, with modes at $\omega/c = 0.45$. Shown are the magnitude (blue solid) and phase (green dash dot) of E (a) and $E^\dagger$ (b) fields and the real (blue solid) and imaginary parts (green dash dot) of the integrands of $\mathcal{N}$ (c) and $\mathcal{F}$ (d) given by (29) and (28).

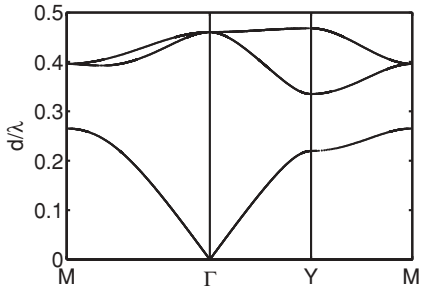

FIG. 4. Band diagram of a 2D periodic structure consisting of a square array dielectric cylinders in vacuum. The index of the cylinders is $n = 3$, and the radius is $a = 0.3d$, where d is the lattice parameter.

The next two examples are 2D examples of a square array of rods in vacuum: (a) an all dielectric structure and (b) a metallic structure. While the structures are 2D, the 1D result of (27) can be applied with an appropriate choice of unit cell. We focus on the dispersion relation in the Γ-X direction. The direction of attenuation in modal fields is also in the Γ-X direction, achieved by analyzing a semi-infinite photonic crystal with a cut plane parallel to the Γ-Y direction.

Band structures were calculated by using a multipole expansion and a transfer matrix method. Fields around each cylinder were expanded in a multipole basis, where analytic expressions were derived for the cylindrical boundary conditions [31]. Lattice sums were used to related the field incoming onto each cylinder to the field outgoing from other cylinders within a single layer of the lattice [32]. The transfer matrix eigenvalue method was applied between the constituent layers of the lattice to produce the band structure [28,33].

Figure 4 shows the band diagram of dielectric rods in vacuum. Figure 5 compares the group velocity, as calculated as $d\omega/dk$ from the band diagram in Fig. 4, and the adjoint field velocity, as calculated from the modal fields, of the Γ-X section. Agreement is found in both the first and second bands, where (27) reduces to the standard definition of energy velocity, and in the band gap, where energy velocity and adjoint field velocity differ.

The third example consists of silver rods in vacuum, which features multiple omnidirectional flat bands at wavelengths around the plasma frequency when loss is neglected [34].

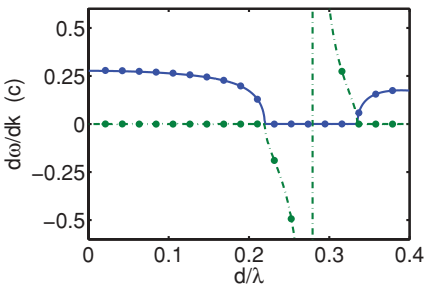

FIG. 5. (Color online) Comparison for the Γ-X segment of the group velocity as calculated from Fig. 4 (lines) and the adjoint field velocity calculated from the modal fields (dots). Blue solid and green dash dot lines denote the real and imaginary parts, respectively. Shown are the first and second bands, where v_g is real, and the band gap, where v_g is purely imaginary.

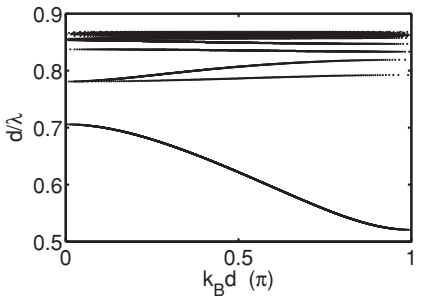

FIG. 6. Band structure of a square array of silver rods in vacuum, with $a = 0.3d$, in the Γ-X direction and loss neglected. Around the plasma frequency, at $d/\lambda \approx 0.87$, a series of flat bands is observed.

A multiresonance Drude-Lorentz model was used to match the optical constants for silver [35]. Figures 6 and 7 shows the Γ-X segment of the band diagram when loss was neglected and when loss was not neglected, respectively. Figure 7 shows the three least lossy modes for each frequency, where loss is quantified by the imaginary part of k. Comparing the lossless and lossy band diagrams, one sees that the flat regions of the band diagram are significantly impacted by loss, demonstrating the importance of loss in the context of Kramers-Kronig-consistent dispersion relations. Figure 8 compares group velocity and adjoint field velocity. Only the least lossy mode is shown. As in the previous examples, numerical agreement is found between group velocity and the adjoint field velocity.

VI. DISCUSSION

When electromagnetic fields lose energy to material absorption, the fields no longer conserve energy. However, the reciprocity theorem remains a valid constraint [36], which is exploited in our construction of the field quantities $\mathcal{F}$ and $\mathcal{N}$ in the definition of the adjoint field velocity. Therefore, the interpretations of $\mathcal{F}$ and $\mathcal{N}$ when loss is present differ from those of the analogous energy velocity quantities of $\langle \boldsymbol{S} \rangle$ and $\langle U \rangle$ when loss is absent. However, these analogous quantities can still be compared within the context of reciprocity and energy conservation. The divergence of time-averaged energy flux $\boldsymbol{S}$ being zero, $\nabla \cdot \mathrm{Re}(\boldsymbol{E} \times \bar{\boldsymbol{H}}) = 0$, is a statement of energy conservation; the divergence of the integrand of $\mathcal{F}$ being zero, $\nabla \cdot (\boldsymbol{E} \times \boldsymbol{H}^{\dagger} - \boldsymbol{E}^{\dagger} \times \boldsymbol{H}) = 0$, is a statement of Lorentz reciprocity. Indeed, it can be shown from the properties of Bloch

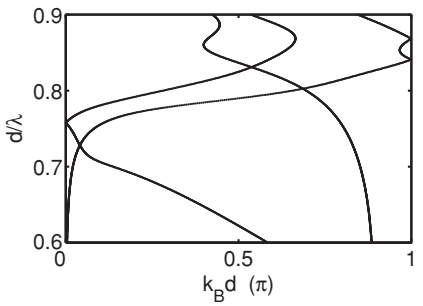

FIG. 7. Same as Fig. 6, but loss is not neglected. Shown are the three least lossy modes.

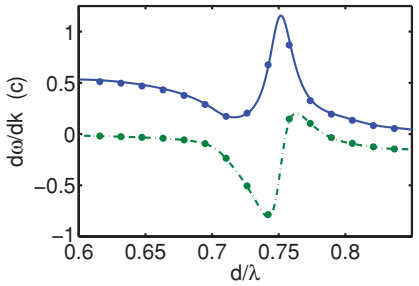

FIG. 8. (Color online) Comparison of the real (blue solid) and imaginary (green dash dot) parts of group velocity (solid lines) and adjoint field velocity (dots) in the Γ-X segment for the bands of Fig. 7. Only the least lossy mode is shown.

modes and their adjoints that this divergence is always zero. Similarly, for $\langle U \rangle$ and $\mathcal{N}$, the time derivative of the integrands being zero are also statements of energy conservation and reciprocity, respectively. Therefore, $\mathcal{F}$ and $\mathcal{N}$ are analogous to $\langle \boldsymbol{S} \rangle$ and $\langle U \rangle$ in the context of reciprocity rather than energy conservation.

The derivation of the energy velocity in Sec. III produces a result that is equivalent to that obtained from $\boldsymbol{k} \cdot \boldsymbol{p}$ perturbation theory [37,38]. In the lossless case, the difference between our derivation and $\boldsymbol{k} \cdot \boldsymbol{p}$ theory is largely immaterial; the meaningful difference arises in the approach to loss. Whereas authors such as Loudon and Sipe include energy transformations from the fields into energy dissipated by the medium [14,39], we turn to adjoint fields. In the context of $\boldsymbol{k} \cdot \boldsymbol{p}$ theory, accounting for all energy transformations preserves Hermiticity of the differential operators that generate the eigenmodes of the system, and Hermiticity is required for the necessary properties of orthonormality and completeness. Using adjoint modes instead considers the dual basis, which provides a complete biorthonormal set of modes. Calculating v_g from the field quantities remains purely an electromagnetic problem, and an explicit model for material characteristics is not required as they are implicitly captured in $\epsilon(\omega)$ and $\mu(\omega)$. In our derivation, we have not explicitly used the completeness and biorthonormality properties, utilizing only the fact that products of modes and adjoint modes possesses the same periodicity as the structure.

Two derivations are presented in this paper relating the complex group velocity to integrals over modal fields. Section III introduces adjoint fields, while Appendix B continues to use complex conjugate fields. Both forms give $d\omega/dk$, but the adjoint field velocity directly gives $d\omega/dk$, while the complex conjugate formulation gives $d\omega/d[\mathrm{Re}(k)]$ and $d\omega/d[\mathrm{Im}(k)]$ separately. The adjoint form is simpler, as extra terms are needed to account for attenuation of modal fields when complex conjugate fields are used. Most significantly, the complex conjugate fields no longer allow two modes on the same band that are infinitesimally separated to be treated as identical to first order. Consequently, to calculate $d\omega/d[\mathrm{Re}(k)]$, calculations of $d\boldsymbol{E}/d[\mathrm{Re}(k)]$ and other similar quantities are explicitly required, a clear disadvantage when compared with the adjoint field velocity.

When loss is present, attenuation is a required feature of the modes. However, the modes may have either ω or k being complex, corresponding to temporal and spatial attenuation, respectively. The adjoint field velocity can handle both such modes, or even modes where both ω and k are complex. The adjoint field velocity is different in these two situations, owing to the differing field distributions. This dictates that the complex group velocity, and hence the dispersion relation, varies markedly depending on whether ω or k is complex. For example, group velocity, in particular $d\omega/d[\mathrm{Re}(k)]$, is significantly impacted by loss at the small group velocity regions of the band in the complex k but not in the complex ω band diagram. However, there is no inconsistency, as complex ω and complex k modes are relevant to different physical situations.

In this paper, we have considered only the adjoint field velocity in 1D, which can be applied to structures periodic in 2D or 3D under limited circumstances. Extensions of the definition to higher dimensions are possible. The dimensionality of the structure affects only the adjoint flux, $\mathcal{F}$, as it is a vector quantity. Generalizations of $\mathcal{F}$ will project the integrand of $\mathcal{F}$ in the direction of a vector $\boldsymbol{k}$ and integrate over the entire unit cell rather than along a single boundary.

VII. CONCLUSION

We have introduced a velocity termed the adjoint field velocity that reproduces the group velocity in lossy media and is calculated from modal field distributions. The adjoint field velocity reduces to the energy velocity in modes of lossless media that do not show attenuation. In lossy media, where the energy velocity differs from the group velocity, the adjoint field velocity remains linked to the group velocity. Thus the adjoint field velocity provides the link between the slope of the dispersion relation and the modal field distribution. In addition to lossy media, the adjoint field velocity is valid whenever the modes of the system have a complex ω or complex k, as in evanescent modes in the band gap of a photonic crystal. Examples are provided to demonstrate the numerical agreement with the group velocity. The results derived are for the 1D case, applying to structures with periodicity in 1D, or structures with infinite translational symmetry in at least 1D. In restricted cases, the results can be applied to structures periodic in 2D or 3D, specifically, when the direction of spatial field attenuation coincides with propagation of energy. Any symmetries present within the structure can be used to obtain the adjoint fields, and thus only one set of modes need be explicitly calculated.

ACKNOWLEDGMENTS

A.A. Asatryan aknowledges support from the Australian Research Council through the Discovery Projects program.

APPENDIX A: BRIEF INTRODUCTION TO ADJOINT MODES

We provide a brief introduction to the adjoint modes and restate some key results of [24] relevant to this paper.

Modes of periodic systems are eigenfunctions of the operator

$$\frac{1}{\mu}\nabla \times \left(\frac{1}{\epsilon}\nabla \times \boldsymbol{H}\right) = \omega^2 \boldsymbol{H}, \tag{A1}$$

which is expressed abstractly as

$$Lu_i = \beta_i u_i, \tag{A2}$$

where β_i is the eigenvalue of the ith mode u_i. Adjoint modes satisfy a similar eigenvalue equation,

$$L^\dagger u_i^\dagger = \beta_i^\dagger u_i^\dagger, \tag{A3}$$

where $u_i^\dagger$ is the ith eigenmode of a yet to be defined adjoint operator $L^\dagger$. An inner product may be defined on the set of all eigenmodes u_i and $u_i^\dagger$,

$$\langle u_i^\dagger, u_j \rangle = \int \boldsymbol{H}_i^\dagger \cdot \boldsymbol{H}_j \, d\boldsymbol{x}. \tag{A4}$$

The adjoint operator, $L^\dagger$, may be defined such that its eigenmodes, $u_i^\dagger$, satisfy the orthonormality condition under an inner product,

$$\langle u_i^\dagger, u_j \rangle = \delta_{ij}, \tag{A5}$$

where δ is the Kronecker delta. Where the operator L is Hermitian,

$$\langle Lu_i^\dagger, u_j \rangle = \langle u_i^\dagger, Lu_j \rangle, \tag{A6}$$

adjoint fields are given by the familiar complex conjugation operation and the adjoint eigenvalue equation (A3) may be reduced to [25]

$$L\bar{u}_i = \beta_i \bar{u}_i. \tag{A7}$$

However, when the operator L is not Hermitian, the eigenmodes obtained from (A7) no longer satisfy the orthonormality condition. Botten *et al.* show in the context of lossy lamellar gratings that defining $u_i^\dagger$ as the set of modes counterpropagating to u_i satisfies the orthonormality condition. These modes have the properties

$$\boldsymbol{E}^\dagger(\boldsymbol{x},\omega,\boldsymbol{k},\epsilon,\mu) = \boldsymbol{E}(\boldsymbol{x},\omega,-\boldsymbol{k},\epsilon,\mu). \tag{A8}$$

It is the property of adjoint modes that $\boldsymbol{k} \to -\boldsymbol{k}$ which we specifically utilize in this paper.

APPENDIX B: COMPLEX GROUP VELOCITY WITHOUT ADJOINT FIELDS

We derive the form of $\mathcal{F}$ and $\mathcal{N}$ in a dispersive and lossy medium using the complex conjugate fields. We begin with

$$\begin{aligned}
\nabla\cdot(\boldsymbol{E_1}\times\bar{\boldsymbol{H}}_2) &= +i\omega_1\mu_1\boldsymbol{H_1}\cdot\bar{\boldsymbol{H}}_2 - i\bar{\omega}_2\bar{\epsilon}_2\boldsymbol{E_1}\cdot\bar{\boldsymbol{E}}_2,\\
-\nabla\cdot(\boldsymbol{E_2}\times\bar{\boldsymbol{H}}_1) &= -i\omega_2\mu_2\bar{\boldsymbol{H}}_1\cdot\boldsymbol{H_2} + i\bar{\omega}_1\bar{\epsilon}_1\bar{\boldsymbol{E}}_1\cdot\boldsymbol{E_2},\\
-\nabla\cdot(\bar{\boldsymbol{E}}_1\times\boldsymbol{H_2}) &= +i\bar{\omega}_1\bar{\mu}_1\bar{\boldsymbol{H}}_1\cdot\boldsymbol{H_2} - i\omega_2\epsilon_2\bar{\boldsymbol{E}}_1\cdot\boldsymbol{E_2},\\
\nabla\cdot(\bar{\boldsymbol{E}}_2\times\boldsymbol{H_1}) &= -i\bar{\omega}_2\bar{\mu}_2\boldsymbol{H_1}\cdot\bar{\boldsymbol{H}}_2 + i\omega_1\epsilon_1\boldsymbol{E_1}\cdot\bar{\boldsymbol{E}}_2,
\end{aligned} \tag{B1}$$

where the four identities may be obtained by a combination of swapping indexes, complex conjugation, or multiplying by -1. As before, we add the four equations. In this derivation, we assume ω is real and k is complex. The corresponding result for complex ω follows by not assuming $\omega = \bar{\omega}$. The right-hand side may be simplified by expanding both $\omega_2\epsilon_2$ and $\boldsymbol{E_2}$ in a Taylor series, neglecting the second-order terms. After integration, the right-hand side is

$$\begin{aligned}
2i(\omega_1-\omega_2)\int_{\mathrm{UC}}\Bigg[&\frac{d(\epsilon_r\omega)}{d\omega}|\boldsymbol{E}|^2 + 2\omega\epsilon_i\mathrm{Im}\left(\boldsymbol{E}\cdot\frac{\partial\bar{\boldsymbol{E}}}{\partial\omega}\right)\\
&+\frac{d(\mu_r\omega)}{d\omega}|\boldsymbol{H}|^2 + 2\omega\mu_i\mathrm{Im}\left(\boldsymbol{H}\cdot\frac{\partial\bar{\boldsymbol{H}}}{\partial\omega}\right)\Bigg]d\boldsymbol{x},
\end{aligned} \tag{B2}$$

where subscripts r and i denote the real and imaginary parts of ϵ and μ. In the absence of loss, this reduces to

$$2i(\omega_1-\omega_2)\int_{\mathrm{UC}}\left[\frac{d(\epsilon\omega)}{d\omega}|\boldsymbol{E}|^2 + \frac{d(\mu\omega)}{d\omega}|\boldsymbol{H}|^2\right]d\boldsymbol{x}, \tag{B3}$$

which justifies the assumption in (18) that $\boldsymbol{E_1} = \boldsymbol{E_2}$ to first order. On the LHS, we obtain, after integrating over the unit cell and using Bloch's theorem to express fields on opposing sides of the unit cell,

$$\begin{aligned}
\mathrm{LHS} &= \int_{\mathrm{L}}\mathrm{Im}\left[(\boldsymbol{E_1}\times\bar{\boldsymbol{H}}_2 + \bar{\boldsymbol{E}}_2\times\boldsymbol{H_1})\right.\\
&\quad\left.\times(e^{i(k_1'-k_2')l}e^{-(k_1''+k_2'')l}-1)\right]\cdot\hat{\boldsymbol{n}}\,ds\\
&\approx\int_{\mathrm{L}}\mathrm{Im}\left[(\boldsymbol{E_1}\times\bar{\boldsymbol{H}}_2 + \bar{\boldsymbol{E}}_2\times\boldsymbol{H_1})\{[1+i(k_1'-k_2')l]\right.\\
&\quad\left.\times e^{-(k_1''+k_2'')l}-1\}\right]\cdot\hat{\boldsymbol{n}}\,ds,
\end{aligned} \tag{B4}$$

introducing the notation $k' = \mathrm{Re}[k]$ and $k'' = \mathrm{Im}[k]$. Expanding $\boldsymbol{E_2}$ and $\boldsymbol{H_2}$ in powers of $(k_2' - k_1')$ and dropping second-order terms gives

$$\begin{aligned}
\mathrm{LHS} = (k_1'-k_2')\int_{\mathrm{L}}\Bigg[&\mathrm{Re}(\boldsymbol{E_1}\times\bar{\boldsymbol{H}}_1)le^{-(k_1''+k_2'')l}\\
&-\mathrm{Im}\left(\boldsymbol{E_1}\times\frac{\partial\bar{\boldsymbol{H}}_1}{\partial k'} + \frac{\partial\bar{\boldsymbol{E}}_1}{\partial k'}\times\boldsymbol{H_1}\right)(e^{-(k_1''+k_2'')l}-1)\Bigg]\cdot\hat{\boldsymbol{n}}ds.
\end{aligned} \tag{B5}$$

Again, setting k_1'' and k_2'' to 0 gives an expression equivalent to (18). Equating the left- and right-hand sides and allowing $\frac{\Delta\omega}{\Delta k'} \to \frac{d\omega}{dk'}$ gives

$$\frac{\partial\omega}{\partial k'} = \frac{l\mathcal{F}}{\mathcal{N}}, \tag{B6}$$

where

$$\begin{aligned}
\mathcal{N} = \int_{\mathrm{UC}}\Bigg[&\frac{d(\epsilon_r\omega)}{d\omega}|\boldsymbol{E}|^2 + 2\omega\epsilon_i\mathrm{Im}\left(\boldsymbol{E}\cdot\frac{\partial\bar{\boldsymbol{E}}}{\partial\omega}\right) + \frac{d(\mu_r\omega)}{d\omega}|\boldsymbol{H}|^2\\
&+2\omega\mu_i\mathrm{Im}\left(\boldsymbol{H}\cdot\frac{\partial\bar{\boldsymbol{H}}}{\partial\omega}\right)\Bigg]d\boldsymbol{x}
\end{aligned} \tag{B7}$$

and

$$\begin{aligned}
\mathcal{F} = \int_{\mathrm{L}}\Bigg[&\mathrm{Re}\,(\boldsymbol{E}\times\bar{\boldsymbol{H}})le^{-2k''l} - \mathrm{Im}\left(\boldsymbol{E}\times\frac{d\bar{\boldsymbol{H}}}{dk'} + \frac{d\bar{\boldsymbol{E}}}{dk'}\times\boldsymbol{H}\right)\\
&\times(e^{-2k''l}-1)\Bigg]\cdot\hat{\boldsymbol{n}}\,ds.
\end{aligned} \tag{B8}$$

The quantity $d\omega/dk''$ can also be obtained by considering a change in sign of two of the four identities in (B1).

[1] S. A. Maier, M. D. Friedman, P. E. Barclay, and O. Painter, Appl. Phys. Lett. **86**, 071103 (2005).
[2] E. Ozbay, Science **311**, 189 (2006).
[3] J. A. Dionne, L. A. Sweatlock, H. A. Atwater, and A. Polman, Phys. Rev. B **72**, 075405 (2005).
[4] E. N. Economou, Phys. Rev. **182**, 539 (1969).
[5] S. Hughes, L. Ramunno, J. F. Young, and J. E. Sipe, Phys. Rev. Lett. **94**, 033903 (2005).
[6] J. G. Pedersen, S. Xiao, and N. A. Mortensen, Phys. Rev. B **78**, 153101 (2008).
[7] A. Reza, M. M. Dignam, and S. Hughes, Nature (London) **455**, E10 (2008).
[8] K. L. Tsakmakidis, A. D. Boardman, and O. Hess, Nature (London) **450**, 397 (2007).
[9] L. Solymar and E. Shamonina, *Waves in Metamaterials* (Oxford University Press, New York, 2009).
[10] L. Brillouin, *Wave Propagation and Group Velocity* (Academic Press, New York, 1960).
[11] R. Y. Chiao, Phys. Rev. A **48**, R34 (1993).
[12] C. G. B. Garrett and D. E. McCumber, Phys. Rev. A **1**, 305 (1970).
[13] A. Yariv and P. Yeh, Phys. Lett. **28**, 735 (1976).
[14] R. Loudon, J. Phys. A **3**, 450 (1970).
[15] S. Chu and S. Wong, Phys. Rev. Lett. **48**, 738 (1982).
[16] L. J. Wang, A. Kuzmich, and A. Dogariu, Nature (London) **406**, 277 (2000).
[17] G. Dolling, C. Enkrich, M. Wegener, C. M. Soukoulis, and S. Linden, Science **312**, 892 (2006).
[18] R. W. Ziolkowski, Phys. Rev. E **63**, 046604 (2001).
[19] G. C. Sherman and K. E. Oughstun, J. Opt. Soc. Am. B **12**, 229 (1995).
[20] K. A. Connor and L. B. Felsen, Proc. IEEE **62**, 1586 (1974).
[21] J. Peatross, S. A. Glasgow, and M. Ware, Phys. Rev. Lett. **84**, 2370 (2000).
[22] A. D. Boardman and K. Marinov, Phys. Rev. B **73**, 165110 (2006).
[23] R. Ruppin, Phys. Lett. A **299**, 309 (2002).
[24] L. C. Botten, M. S. Craig, R. C. McPhedran, J. L. Adams, and J. R. Andrewartha, J. Mod. Opt. **28**, 1087 (1981).
[25] J. D. Joannopoulos, S. G. Johnson, and J. N. Winn, *Photonic Crystals: Molding the Flow of Light* (Princeton University Press, Princeton, NJ, 2008).
[26] P. M. Morse and H. Feshbach, *Methods of Theoretical Physics* (McGraw-Hill, New York, 1953), Vol. 1, pp. 869–886.
[27] A. L. Burin, M. A. Ratner, H. Cao, and R. P. H. Chang, Phys. Rev. Lett. **87**, 215503 (2001).
[28] L. C. Botten, N. A. Nicorovici, R. C. McPhedran, C. M. Sterke, and A. A. Asatryan, Phys. Rev. E **64**, 046603 (2001).
[29] J. D. Jackson, *Classical Electrodynamics* (Wiley, New York, 1998).
[30] P. Yeh and M. Hendry, *Optical Waves in Layered Media* (Wiley, New York, 1988).
[31] L. C. Botten, N. A. P. Nicorovici, A. A. Asatryan, R. C. McPhedran, C. Martijn de Sterke, and P. A. Robinson, J. Opt. Soc. Am. A **17**(12), 2177 (2000).
[32] R. C. McPhedran, N. A. Nicorovici, L. C. Botten, and K. A. Grubits, J. Math. Phys. **41**, 7808 (2000).
[33] K. Dossou, M. A. Byrne, and L. C. Botten, J. Comput. Phys. **219**, 120 (2006).
[34] A. R. McGurn and A. A. Maradudin, Phys. Rev. B **48**, 17576 (1993).
[35] A. D. Rakic, A. B. Djurisic, J. M. Elazar, and M. L. Majewski, Appl. Opt. **37**, 5271 (1998).
[36] D. Maystre and R. C. McPhedran, Opt. Commun. **12**, 164 (1974).
[37] N. A. R. Bhat and J. E. Sipe, Phys. Rev. E **64**, 056604 (2001).
[38] C. Kittel, *Quantum Theory of Solids* (Wiley, New York, 1963).
[39] N. A. R. Bhat and J. E. Sipe, Phys. Rev. A **73**, 063808 (2006).